

AWACS Radar Aircraft Trajectory Tracking via Networked Ground Receiver Stations

Michel Kulhandjian[†], Hovannes Kulhandjian[‡] and Ashutosh Sabharwal[†]

[†]Department of Electrical and Computer Engineering, Rice University, Houston, TX USA

E-mail: {mk120, ashu}@rice.edu

[‡]Department of Electrical and Computer Engineering, California State University, Fresno, CA USA

E-mail: hkulhandjian@mail.fresnostate.edu

Abstract—In this paper, we study the tracking of an airborne warning and control system (AWACS) radar position using receptions from a network of ground receiver stations. We demonstrate that combining received signal strength from each of the networked participating receivers can enable accurate trajectory tracking. We propose a localization estimator integrates maximum-likelihood-based angle of arrival and triangulation methods. The proposed scheme circumvents the challenges associated with trilateration-based tracking algorithms, where the placement of receivers is critical to avoid ill-conditioned matrices. Simulation results demonstrate a 100-fold improvement in accuracy at an SNR of 16 dB compared to RSSI-based estimators.

I. INTRODUCTION

The airborne warning and control system (AWACS) developed by Boeing is a radar system specifically designed to detect a wide array of targets, including aircraft, ships, vehicles, missiles, and other incoming projectiles, at considerable distances. Its primary function lies in commanding and controlling the battlespace during air engagements by directing fighter and attack aircraft strikes. AWACS conducts essential surveillance operations, such as the detection and tracking of targets, contributing to the identification of friendly or hostile entities. Notably, AWACS boasts an extended tracking coverage compared to its ground-based radar counterparts. However, like other airborne systems, AWACS is susceptible to various malicious attacks, including cyber threats and passive tracking of critical aircraft locations.

This paper delves into the exploration of an exposed vulnerability related to tracking the trajectory of an AWACS system. We investigate this vulnerability by examining the received signals from a *network* of ground stations, such as a network of cellular base stations sharing spectrum with the radar. Given their nationwide deployment, these ground stations have the potential to track an AWACS carrier over extensive trajectories.

Our contributions unfold in two primary aspects. Firstly, we model the AWACS airborne system with a transmitting rotodome and trajectory tracking, utilizing a network of radar receivers. This becomes particularly crucial as the spectrum used by AWACS is shared with commercial cellular systems like citizens broadband radio service (CBRS). Secondly, we introduce a maximum-likelihood (ML) approach and a comparison with other existing algorithms. We perform a simulation-based evaluation of the proposed method by varying the number of receivers deployed on the ground in a two-dimensional grid. We model the aircraft position and assess the precision of tracking by varying the number of received

nodes and signal-to-noise ratio (SNR) values. The results of the simulations demonstrate that our proposed trajectory tracking scheme exhibits enhanced error performance compared to RSSI-based schemes with an increased number of receiving nodes. Specifically, we achieve a remarkable 100-fold improvement in error at an SNR of 16 dB.

The remainder of this paper is organized as follows. In Section II, we provide an overview of related work, followed by the presentation of the system model and problem formulation in Section III. RSSI and AoA-based methods are detailed in Sections IV and V, respectively. Our experimental setup is described, and trajectory tracking precision analysis is discussed in Section VI. Finally, we conclude our findings in Section VII.

II. RELATED WORK

Location estimation holds significant importance in both military and civilian applications, gaining prominence in the field of wireless communications. Generally, localization approaches are broadly classified into range-based and range-free schemes. Range-based localization methods aim to estimate physical distance or relative angles between nodes by leveraging various localization measurements, including received signal strength indicator (RSSI) [1], time of arrival (ToA) [2], time difference of arrival (TDoA) [3], frequency difference of arrival (FDoA) [4], and angle of arrival (AoA) [5]. Among these, RSSI is the most commonly used method, given that many radio frequency (RF) wireless devices come equipped with built-in RSSI capabilities, allowing for measurement without additional cost. However, the accuracy of RSSI-based schemes is compromised due to factors such as noise, interference, multipath fading, and challenges in approximating a common propagation model in varying environmental channel conditions. Contrastingly, other range-based localization schemes like ToA, TDoA, and AoA often require additional specialized hardware (e.g., smart antenna arrays) or increased computing resources to obtain accurate distance or angle measurements. Range-free methods, while cost-effective, generally exhibit lower accuracy compared to their range-based counterparts.

In this article, our focus is on range-based methods, specifically examining their accuracy over different channel conditions. The study aims to provide insights into the challenges and potentials of range-based localization methods in various wireless communication scenarios.

III. SYSTEM MODEL AND PROBLEM FORMULATION

A. Radar Transmitter

In a typical AWACS airborne, an array of transmitting antennas in the rotodome undergoes about six revolutions per minute (rpm) during operation. Let the pulsed linear frequency-modulated (LFM) waveforms transmitted at each antenna are represented by

$$s(t) = \sum_{p=0}^{P-1} x(t - \tau - pT) \Pi\left(\frac{t - \tau - pT}{\Omega}\right), \quad (1)$$

where P is the number of pulses, τ is an initial sample delay from the start of the first pulse, and T is the pulse repetition interval. The function $\Pi(\cdot)$ is defined as a rectangular indicator function where

$$\Pi\left(\frac{t}{\Omega}\right) = \begin{cases} 1 & t \leq \Omega \\ 0 & t > \Omega \end{cases}, \quad (2)$$

and the component pulse $x(t)$ is given as

$$x(t) = A e^{j(\phi_0 + 2\pi f t \Delta + \pi g (t \Delta)^2)}. \quad (3)$$

Here A is the amplitude of the pulse, ϕ_0 is an initial phase offset, f is the starting frequency, and g is the *chirp rate* defined as $g = B/\Omega$ Hz/s, where B is the pulse bandwidth and Ω is the pulse duration.

The radiation of the radar signal from the rotating transmit antenna arrays can be modeled as a rotating plane in 3-D as follows,

$$\mathbf{X}(t) = \mathbf{R}(t) \mathbf{A} s(t) \in \mathbb{C}^{3 \times K}, \quad (4)$$

where $\mathbf{R}(t)$ is the transformation via axis rotation in elevation and azimuth angles, $\theta'(t)$, $\phi'(t)$, in 3-D as

$$\mathbf{R}(t) = \begin{bmatrix} \cos \theta'(t) \cos \phi'(t) & \cos \theta'(t) \sin \phi'(t) & -\sin \theta'(t) \\ -\sin \phi'(t) & \cos \phi'(t) & 0 \\ \sin \theta'(t) \cos \phi'(t) & \sin \theta'(t) \sin \phi'(t) & \cos \theta'(t) \end{bmatrix}, \quad (5)$$

\mathbf{A} models the 2-D plane of the antenna array of rotodome in 3-D,

$$\mathbf{A} = \left[\mathbf{p}_1 e^{j \frac{2\pi}{\lambda} \mathbf{u}^T \mathbf{p}_1} \quad \dots \quad \mathbf{p}_K e^{j \frac{2\pi}{\lambda} \mathbf{u}^T \mathbf{p}_K} \right] \in \mathbb{C}^{3 \times K}, \quad (6)$$

where \mathbf{p}_k is the k -th radiating antenna position,

$$\mathbf{p}_i = [x_k, y_k, z_k]^T \in \mathbb{R}^{3 \times 1}, \quad (7)$$

and the steering vector of the antenna array is

$$\mathbf{u} = [\sin \theta_t \cos \phi_t, \sin \theta_t \sin \phi_t, \cos \theta_t]^T, \quad (8)$$

where θ_t and ϕ_t are steering elevation and azimuth angles of the rotodome respectively, and K is the number of antenna elements in the array.

B. Network Receivers

We study the receiver network nodes that are placed in a uniform grid-like plane and airborne radar will be flying over the region as depicted in Fig. 1.

For simplicity, in our study, we assume that there is a single radar source, denoted as $s(t)$, emitting signals from a 2-D antenna array on an airborne platform moving at a constant

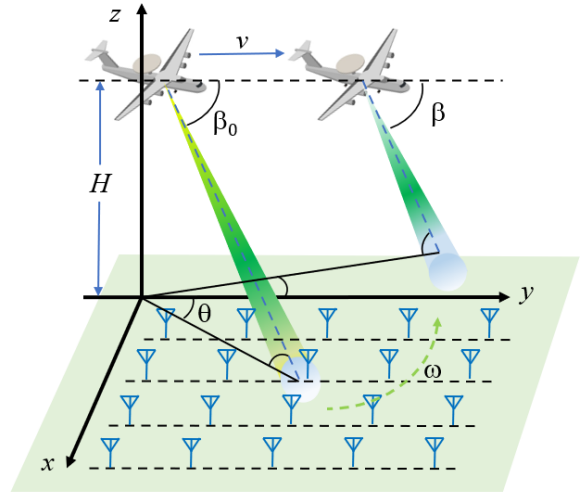


Fig. 1: Angular scanning of AWACS radar across a network of ground receiving nodes.

velocity in a multipath-free environment with constant scanning angular velocity, ω . We will position M multiple-input multiple-output (MIMO) receiving nodes within a specified terrain, as illustrated in Fig. 2.

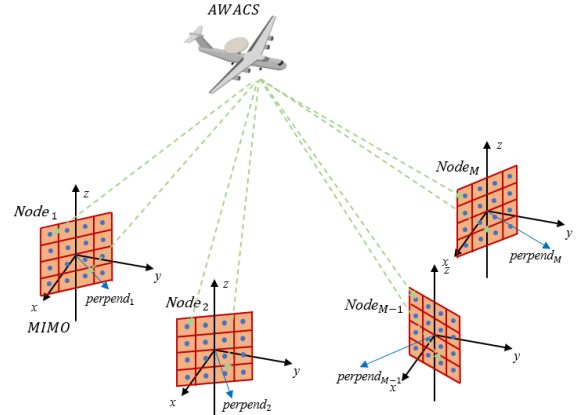


Fig. 2: Ground nodes passively receive the radar signal from AWACS, equipped with MIMO antennas.

The received signal $r_{m,k}(t)$ at the m -th receiving node and k -th antenna in baseband can be written as

$$r_{m,k}(t) = \alpha'_m a_k(\theta_m, \phi_m) s'(t - \tau_m) e^{j2\pi f_m t} + n_{m,k}(t), \quad (9)$$

where α'_m denotes an unknown scaling coefficient that accounts for both the antenna gain and channel propagation effects, $a_k(\theta_m, \phi_m)$ is the steering coefficient of k -th antenna with received elevation and azimuth angles, θ_m and ϕ_m , $s'(t)$ represents the radar source signal given by (1), τ_m is the propagation delay, f_m is the Doppler frequency, and $n_m(t)$ is characterized as temporally and spatially white mutually uncorrelated circular complex Gaussian noise with a zero mean. We designate receiving node 1 as the reference

node, having the strongest observed signal among M nodes. Consequently, we express parameters relative to node 1, such as $\tau_{m1} \triangleq \tau_m - \tau_1$ and $f_{m1} \triangleq f_m - f_1$. Additionally, we introduce the definitions:

$$s(t) \triangleq s'(t - \tau_1)e^{j2\pi f_1 t}, \quad (10)$$

and

$$\alpha_m \triangleq \alpha'_m e^{j2\pi f_1 \tau_{m1}}. \quad (11)$$

It can be shown that (9) can be reformulated as

$$r_{m,k}(t) = \alpha_m a_k(\theta_m, \phi_m) s(t - \tau_{m1}) e^{j2\pi f_{m1} t} + n_{m,k}(t), \quad (12)$$

and in vector form as

$$\mathbf{r}_m(t) = \alpha_m \mathbf{a}(\theta_m, \phi_m) s(t - \tau_{m1}) e^{j2\pi f_{m1} t} + \mathbf{n}_m(t) \in \mathbb{C}^{K' \times 1}, \quad (13)$$

where K' is the number of received antenna elements. Moreover, given our assumption of the radar signal as a narrowband signal, we can approximate

$$s(t) \approx s(t - \tau_{m1}), \quad (14)$$

for $1 \leq m \leq M$ and define $\bar{\alpha}_m \triangleq \alpha_m e^{j2\pi f_{m1} t}$. Consequently, (13) can be rewritten as

$$\mathbf{r}_m(t) = \bar{\alpha}_m \mathbf{a}(\theta_m, \phi_m) s(t) + \mathbf{n}_m(t) \in \mathbb{C}^{K' \times 1}. \quad (15)$$

The received steering vector, denoted as $\mathbf{a}(\theta_m, \phi_m)$, is contingent upon the configuration of the antenna array. Let's consider the scenario where each receiving nodes is equipped with a $K_y \times K_x$ element uniform rectangular array (URA), resulting in a total number of antenna elements $K' = K_x K_y$. In this setup, the array elements lie in the x-y plane and are spaced by d_x in the x-direction and d_y in the y-direction. For a transmitted radar far-field narrowband signal impinging on the URA with elevation and azimuth angles θ_m and ϕ_m for the m -th receiving node, the received steering vector can be represented as

$$\mathbf{a}(\theta_m, \phi_m) = [\mathbf{a}_y(\theta_m, \phi_m) \otimes \mathbf{a}_x(\theta_m, \phi_m)] \in \mathbb{C}^{K' \times 1}, \quad (16)$$

where \otimes denotes the Kronecker product, and $\mathbf{a}_y(\theta_m, \phi_m)$ and $\mathbf{a}_x(\theta_m, \phi_m)$ represent the steering vectors along the y-axis and x-axis, respectively,

$$\begin{aligned} \mathbf{a}_y(\theta_m, \phi_m) &= [1, e^{j\psi_{y,m}}, \dots, e^{j\psi_{y,m}(K_y-1)}]^T \in \mathbb{C}^{K_y \times 1} \\ \mathbf{a}_x(\theta_m, \phi_m) &= [1, e^{j\psi_{x,m}}, \dots, e^{j\psi_{x,m}(K_x-1)}]^T \in \mathbb{C}^{K_x \times 1}. \end{aligned}$$

The phase terms $\psi_{y,m}$ and $\psi_{x,m}$ are expressed as

$$\psi_{y,m} = \frac{2\pi}{\lambda} d_y \sin \theta_m \sin \phi_m \quad (17)$$

$$\psi_{x,m} = \frac{2\pi}{\lambda} d_x \sin \theta_m \cos \phi_m, \quad (18)$$

where λ represents the signal wavelength.

IV. RSSI-BASED LOCALIZATION

The RSSI-based scheme is typically cost-effective, as it does not necessitate additional hardware and can be deployed as a network of single-antenna receivers.

A. Trilateration Algorithm

One of the basic position estimation schemes is the trilateration algorithm, which is widely used in practice [6] [7]. The algorithm requires to have at least three receiver nodes for positioning the target. The relationship between the aircraft and the three receiver nodes can be expressed as

$$\begin{aligned} (x - x_1)^2 + (y - y_1)^2 + (z - z_1)^2 &= d_1^2 \\ (x - x_2)^2 + (y - y_2)^2 + (z - z_2)^2 &= d_2^2 \\ (x - x_3)^2 + (y - y_3)^2 + (z - z_3)^2 &= d_3^2 \end{aligned}$$

where (x, y, z) are the coordinates of the aircraft and (x_1, y_1, z_1) , (x_2, y_2, z_2) , and (x_3, y_3, z_3) are the coordinates of the three receiver nodes. To express the formulation in a matrix, we can rewrite it as follows $\mathbf{Q}\mathbf{x} = \mathbf{b}$, where $\mathbf{Q} \in \mathbb{R}^{3 \times 3}$ and it is defined as

$$\mathbf{Q} = 2 \begin{bmatrix} (x_1 - x_2) & (y_1 - y_2) & (z_1 - z_2) \\ (x_1 - x_3) & (y_1 - y_3) & (z_1 - z_3) \\ (x_2 - x_3) & (y_2 - y_3) & (z_2 - z_3) \end{bmatrix}, \quad (19)$$

and vector $\mathbf{b} \in \mathbb{R}^{3 \times 1}$ is defined as

$$\mathbf{b} = \begin{bmatrix} (x_1^2 - x_2^2) + (y_1^2 - y_2^2) + (z_1^2 - z_2^2) + d_2^2 - d_1^2 \\ (x_1^2 - x_3^2) + (y_1^2 - y_3^2) + (z_1^2 - z_3^2) + d_3^2 - d_1^2 \\ (x_2^2 - x_3^2) + (y_2^2 - y_3^2) + (z_2^2 - z_3^2) + d_3^2 - d_2^2 \end{bmatrix}. \quad (20)$$

Consequently, the estimated aircraft position is given by

$$\hat{\mathbf{x}} = \mathbf{Q}^{-1} \mathbf{b}, \quad (21)$$

where $\hat{\mathbf{x}}$ is the estimated aircraft coordinates. The solution of (21) exist if and only if the determinant of \mathbf{Q} is non-zero. In practical scenarios, the terrain is not perfectly flat, leading to variations in the z-coordinate. This introduces ill-conditioning in \mathbf{Q} , thereby causing increased errors in the estimation process.

B. Tetrahedron-based Algorithm

In this section, we describe the tetrahedron-based algorithm which is based on three distances $d_1 \leq d_2 \leq d_3$, and the angle θ between the receiver nodes corresponding to d_1 and d_2 , respectively. Let all the networked ground receivers be stationed anywhere on the x-y plane. The distances between receiving nodes and the target are calculated by using the RSSIs. After selecting the shortest distances $d_1 \leq d_2 \leq d_3$, as depicted in Fig. 3, we apply the law of cosine and Heron's formula to the tetrahedron for computing the aircraft's position coordinates. Let

$$a_{12} = \frac{r_{12}^2 + d_1^2 - d_2^2}{2r_{12}}, \quad (22)$$

$$a_{13} = \frac{r_{13}^2 + d_1^2 - d_3^2}{2r_{13}}, \quad (23)$$

$$\cos \theta = \frac{r_{12}^2 + r_{12}^2 - r_{23}^2}{2r_{12}r_{13}}, \quad (24)$$

where r_{ij} is the distance between receiver nodes corresponding to d_i and d_j distance. To compute the location of the aircraft on the x-y plane using (22) - (24) we have

$$\hat{\mathbf{p}}_{xy} = \mathbf{p}_1 - a_{12} \mathbf{u}_{12} - \frac{a_{13} - a_{12} \cos \theta}{\sin \theta} \mathbf{u}_{12}^-, \quad (25)$$

where \mathbf{p}_i is the coordinate of the receiver node corresponding to d_i , \mathbf{u}_{1i} is the unit vector of $\mathbf{p}_1 - \mathbf{p}_i$, and $\hat{\mathbf{p}}_{xy}$ is the estimated target position on x-y plane of the receiver nodes. The \mathbf{u}_{12}^- is the orthogonal to \mathbf{u}_{12} and is defined as

$$\mathbf{u}_{12}^- = \begin{bmatrix} \cos \alpha & -\sin \alpha \\ \sin \alpha & \cos \alpha \\ 0 & 0 \end{bmatrix} \mathbf{u}_{12}, \quad (26)$$

where

$$\alpha = \begin{cases} \frac{\pi}{2}, & \text{if } u_{12}(1) = 0, u_{12}(2) = 1, u_{13}(1) = 1 \\ & u_{12}(1) = 0, u_{12}(2) = -1, u_{13}(1) = -1 \\ & u_{12}(1) = 1, u_{12}(2) = 0, u_{13}(2) = -1 \\ & u_{12}(1) = -1, u_{12}(2) = 0, u_{13}(1) = 1 \\ -\frac{\pi}{2}, & \text{otherwise} \end{cases}. \quad (27)$$

Therefore, knowing the x and y coordinates, $\hat{\mathbf{p}}_{xy}$, the z coordinate can be expressed as

$$z = \sqrt{d_1^2 - \frac{a_{12}^2 + a_{13}^2 - 2a_{12}a_{13} \cos \theta}{1 - \cos \theta^2}}. \quad (28)$$

The estimated target position can be written as $\hat{\mathbf{p}}_t = \hat{\mathbf{p}}_{xy} + [0, 0, z]^T$.

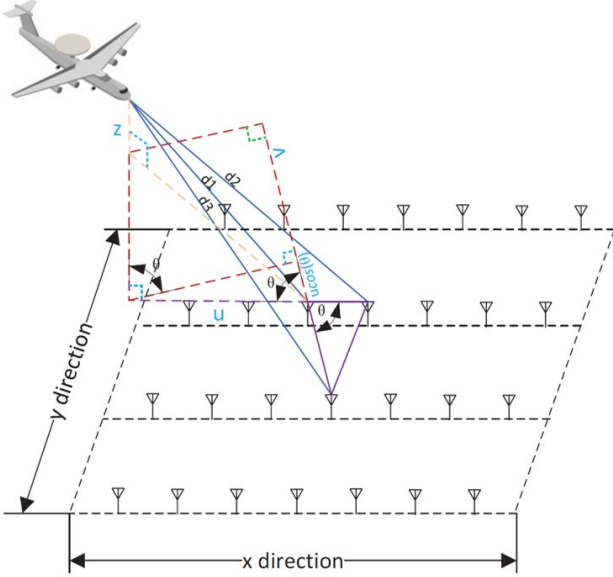


Fig. 3: Trilateration based on Tetrahedron geometry distance relation.

V. AOA-BASED LOCALIZATION

We leverage MIMO receiver diversity as shown in Fig. 2 to derive the AoA at each m -node and subsequently perform triangulation to determine the location. Our approach to addressing this problem adopts an ML perspective. The receiver joint log-likelihood function for the discrete sampled received signal $\mathbf{r} = [\mathbf{r}_1^T[1], \mathbf{r}_1^T[2], \dots, \mathbf{r}_1^T[N], \dots, \mathbf{r}_M^T[1], \mathbf{r}_M^T[2], \dots, \mathbf{r}_M^T[N]]^T$ can be expressed as follows

$$L(\mathbf{r}|\boldsymbol{\theta}, \boldsymbol{\phi}, \boldsymbol{\alpha}, \mathbf{s}, \sigma^2) = \sum_{m=1}^M \sum_{n=1}^N L_n(\mathbf{r}_m[n]|\theta_m, \phi_m, \bar{\alpha}_m, s[n], \sigma^2) \quad (29)$$

where $\mathbf{r}_m[n] \in \mathbb{C}^{K' \times 1}$ denotes the sampled receiver vector at the n -th snapshot of the m -th receiver node, N represents the number of snapshots, $\boldsymbol{\theta} = [\theta_1, \dots, \theta_M]^T$, $\boldsymbol{\phi} = [\phi_1, \dots, \phi_M]^T$, $\boldsymbol{\alpha} = [\bar{\alpha}_1, \dots, \bar{\alpha}_M]^T$, $s[n]$ is the n -th radar signal snapshot, σ^2 denotes the variance of noise in the channel, and $L_n(\mathbf{r}_m[n]|\theta_m, \phi_m, \bar{\alpha}_m, s[n], \sigma^2)$ is defined as

$$L_n(\mathbf{r}_m[n]|\theta_m, \phi_m, \bar{\alpha}_m, s[n], \sigma^2) = -\frac{K'}{2} (\ln 2\pi + \ln \sigma^2) - \frac{1}{2\sigma^2} \|\mathbf{r}_m[n] - \bar{\alpha}_m \mathbf{a}(\theta_m, \phi_m) s[n]\|^2.$$

The objective of ML estimator is to maximize (29). We estimate $\bar{\alpha}_m$ by taking the derivative of (29) with respect to $\bar{\alpha}_m$ and equating the result to zero, and obtaining

$$\hat{\alpha}_m = \frac{\mathbf{r}_m^H[n] \mathbf{a}(\theta_m, \phi_m) s[n]}{|s[n]|^2 \mathbf{a}^H(\theta_m, \phi_m) \mathbf{a}(\theta_m, \phi_m)}, \quad m = 1, 2, \dots, M. \quad (30)$$

Substituting (30) into (29), we obtain

$$L(\mathbf{r}|\boldsymbol{\theta}, \boldsymbol{\phi}, \sigma^2) = -\frac{MNK'}{2} (\ln 2\pi + \ln \sigma^2) - \frac{1}{2\sigma^2} \left(\bar{R} - \sum_{m=1}^M R_m \right), \quad (31)$$

where $\bar{R} = \sum_{m=1}^M \sum_{n=1}^N \|\mathbf{r}_m[n]\|^2$ and

$$R_m = \frac{\mathbf{a}^H(\theta_m, \phi_m) \sum_{n=1}^N \mathbf{r}_m[n] \mathbf{r}_m^H[n] \mathbf{a}(\theta_m, \phi_m)}{\mathbf{a}^H(\theta_m, \phi_m) \mathbf{a}(\theta_m, \phi_m)},$$

respectively. Notably, unknown parameters $\boldsymbol{\alpha}$ and \mathbf{s} has been eliminated in (31). By taking the derivative of (31) with respect to σ^2 and equating to zero, we obtain the following results

$$\hat{\sigma}^2 = \frac{\bar{R} - \sum_{m=1}^M R_m}{MNK'}. \quad (32)$$

Substituting (32) back to (31) and ignoring some constant terms, we obtain

$$L_n(\mathbf{r}|\boldsymbol{\theta}, \boldsymbol{\phi}) = -\frac{MNK'}{2} \ln \left(\bar{R} - \sum_{m=1}^M R_m \right). \quad (33)$$

Therefore, MLE solution of (33) involves maximizing $\sum_{m=1}^M R_m$. Since the maximization is linear and independent of m , the (θ_m, ϕ_m) that maximizes R_m for $1 \leq m \leq M$ is given by

$$\{\hat{\theta}_m, \hat{\phi}_m\} = \arg \max_{\theta_m, \phi_m} \frac{\mathbf{a}^H(\theta_m, \phi_m) \mathbf{R}_m \mathbf{a}(\theta_m, \phi_m)}{\mathbf{a}^H(\theta_m, \phi_m) \mathbf{a}(\theta_m, \phi_m)}, \quad (34)$$

where $\mathbf{R}_m = \sum_{n=1}^N \mathbf{r}_m[n] \mathbf{r}_m^H[n]$. In this problem formulation, the MLE solution (34) aligns with the 2-D multiple signal classification (MUSIC) algorithm [8]. By extending the span of the steering vector $\mathbf{a}(\theta_m, \phi_m)$ to encompass the entire complex space, i.e., $\mathbf{a} \in \mathbb{C}^{K' \times 1}$, maximizing (34) with respect to \mathbf{a} is equivalent to maximizing the Rayleigh quotient. The well-established solution involves identifying the largest eigenvalue achieved by the corresponding eigenvector of the matrix \mathbf{R}_m . In our methodology, we perform a search in the discretized space of elevation and azimuth angles to attain the maximum. Upon estimating θ_m and ϕ_m for $1 \leq m \leq M$, coupled with

the known locations of the nodes, we employ a triangulation algorithm to localize the aircraft. This approach integrates the strengths of the MLE, enabling robust angle estimation, and triangulation techniques for accurate localization based on the acquired angle information.

VI. SIMULATIONS

In this section, we conduct a simulation study with a varying number of receiver nodes positioned on the ground. All receiver nodes are uniformly dispersed, spanning 100 meters across the x and y directions, respectively, at $z = 0$ in a grid-like arrangement. The tracker and aircraft are situated at coordinates $(2, -1.4, 0)$ km and $(2, 2.5, 10)$ km, respectively, with a velocity of 160 m/s. The transmitted LFM pulse has a bandwidth of $B = 4.55$ MHz and a pulse duration of $\Omega = 1.5 \mu\text{s}$, rotating at an angular speed of 3 rpm. Fig. 4 illustrates the performance of different estimation techniques in terms of root mean square error (RMSE) and SNR. For

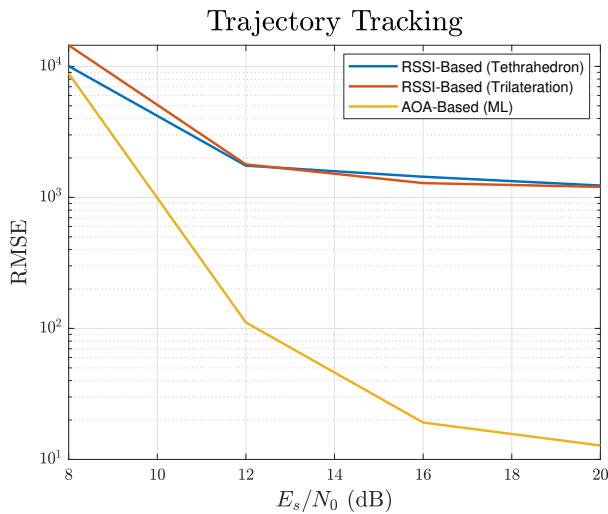


Fig. 4: Accuracy performance in terms of RMSE versus SNR.

the RSSI-based scheme, we assume the receiver nodes have the knowledge of the transmission power, whereas for the AoA-based scheme, we exploit MIMO diversity gain. In this particular configuration, 24 receiver nodes were employed. The appearance of a floor as the SNR increases is attributed to the degradation of the radar signal in the channel. Further simulations were conducted by varying the number of receiver nodes, as depicted in Fig. 5. The results demonstrate that an increase in the number of receiver nodes correlates with a reduction in estimation error.

VII. CONCLUSION

In this paper, we explore the tracking of an AWACS radar's position using signals received from a network of ground receiver stations. This capability holds potential for development using the existing network infrastructure of commercial cellular networks deployed in the CBRS band. Our study includes an analysis of estimation errors to evaluate the precision of the AWACS trajectory. This assessment is conducted by

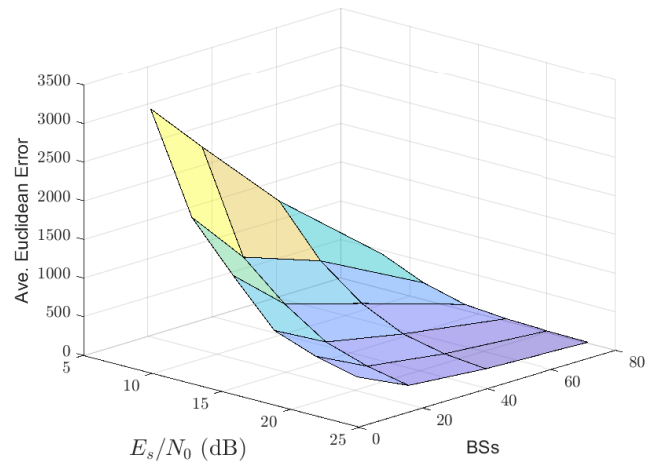


Fig. 5: Accuracy in terms of RMSE by varying the SNR and number of receivers.

varying the number of received nodes and SNR values. Simulation results demonstrate that our proposed trajectory tracking scheme exhibits improved error performance, achieving a 100-fold reduction in errors at an SNR of 16 dB compared with existing RSSI-based schemes. In our future research, we aim to design radar systems geared towards countering the tracking of AWACS planes.

VIII. ACKNOWLEDGEMENT

The work was partially supported by Army Research Labs Cooperative Agreement Number W911NF-19-2-0269.

REFERENCES

- [1] G. Wang and K. Yang, "A new approach to sensor node localization using rssi measurements in wireless sensor networks," *IEEE Trans. on Wireless Commun.*, vol. 10, no. 5, pp. 1389–1395, 2011.
- [2] A. Catovic and Z. Sahinoglu, "The cramer-rao bounds of hybrid toa/rss and tdoa/rss location estimation schemes," *IEEE Commun. Letters*, vol. 8, no. 10, pp. 626–628, 2004.
- [3] F. Shu, S. Yang, J. Lu, and J. Li, "On impact of earth constraint on tdoa-based localization performance in passive multisatellite localization systems," *IEEE Syst. Journal*, vol. 12, no. 4, pp. 3861–3864, 2018.
- [4] H. Yu, G. Huang, J. Gao, and B. Liu, "An efficient constrained weighted least squares algorithm for moving source location using tdoa and fdoa measurements," *IEEE Trans. on Wireless Commun.*, vol. 11, no. 1, pp. 44–47, 2012.
- [5] S. Xu and K. Doğançay, "Optimal sensor placement for 3-d angle-of-arrival target localization," *IEEE Trans. on Aerospace and Electronic Systems*, vol. 53, no. 3, pp. 1196–1211, 2017.
- [6] H. Kulhandjian, M. Kulhandjian, Y. Kim, and C. D'Amours, "2-D DOA Estimation of Coherent Wideband Signals with Auxiliary-Vector Basis," in *Proc. of IEEE Intl. Conf. on Communications (ICC) Workshop on Advances in Network Localization and Navigation (ANLN)*, Kansas City, MO, USA, May 2018, pp. 1–6.
- [7] H. Kulhandjian and T. Melodia, "A Low-cost Distributed Networked Localization and Time-synchronization Framework for Underwater Acoustic Testbeds," in *Proc. of IEEE Underwater Communications Conf. and Workshop (UComms)*, Sestri Levante, Italy, September 2014, pp. 1–5.
- [8] P. Stoica and A. Nehorai, "Music, maximum likelihood, and cramer-rao bound," *IEEE Trans. on Acoustics, Speech, and Signal Proc.*, vol. 37, no. 5, pp. 720–741, 1989.